Geo-Mar Lett (2005) 25: 167–182
DOI 10.1007/s00367-004-0198-6

ORIGINAL

N. N. Romanovskii · H.-W. Hubberten · A. V. Gavrilov
A. A. Eliseeva · G. S. Tipenko

Offshore permafrost and gas hydrate stability zone on the shelf of East Siberian Seas

Received: 28 August 2004 / Accepted: 29 April 2004 / Published online: 9 March 2005

Abstract Dynamics of the submarine permafrost regime, including distribution, thickness, and temporal evolution, was modeled for the Laptev and East Siberian Sea shelf zones. This work included simulation of the permafrost-related gas hydrate stability zone (GHSZ). Simulations were compared with field observations. Model sensitivity runs were performed using different boundary conditions, including a variety of geological conditions as well as two distinct geothermal heat flows (45 and 70 mW/m^2). The heat flows used are typical for the coastal lowlands of the Laptev Sea and East Siberian Sea. Use of two different geological deposits, that is, unconsolidated Cainozoic strata and solid bedrock, resulted in the significantly different magnitudes of permafrost thickness, a result of their different physical and thermal properties. Both parameters, the thickness of the submarine permafrost on the shelf and the related development of the GHSZ, were simulated for the last four glacial-eustatic cycles (400,000 years). The results show that the most recently formed permafrost is continuous to the 60-m isobath; at the greater depths of the outer part of the shelf it changes to discontinuous and "patchy" permafrost. However, model results suggest that the entire Arctic shelf is underlain by relic permafrost in a state stable enough for gas hydrates. Permafrost, as well as the GHSZ, is currently storing probable significant greenhouse gas sources, especially methane that has formed by the decomposition of gas hydrates at greater depth. During climate cooling and associated marine regression, permafrost aggradation takes place due to the low temperatures and the direct exposure of the shelf to the atmosphere. Permafrost degradation takes place during climate warming and marine transgression. However, the temperature of transgressing seawater in contact with the former terrestrial permafrost landscape remains below zero, ranging from −0.5 to −1.8°C, meaning permafrost degradation does not immediately occur. The submerged permafrost degrades slowly, undergoing a transformation in form from ice bonded terrestrial permafrost to ice bearing submarine permafrost that does not possess a temperature gradient. Finally the thickness of ice bearing permafrost decreases from its lower boundary due to the geothermal heat flow. The modeling indicated several other features. There exists a time lag between extreme states in climatic forcing and associated extreme states of permafrost thickness. For example, permafrost continued to degrade for up to 10,000 years following a temperature decline had begun after a climate optimum. Another result showed that the dynamic of permafrost thickness and the variation of the GHSZ are similar but not identical. For example, it can be shown that in recent time permafrost degradation has taken place at the outer part of the shelf whereas the GHSZ is stable or even thickening.

N. N. Romanovskii · A. V. Gavrilov
A. A. Eliseeva · G. S. Tipenko
Faculty of Geology and Faculty of Mathematic and Mechanic,
M.V. Lomonosov Moscow State University, Russia

H.-W. Hubberten (✉)
Alfred Wegener Institute for Polar and Marine Research,
Telegrafenberg A43, 14473 Potsdam, Germany
E-mail: hubbert@awi-potsdam.de
Tel.: +49-331-2882100
Fax: +49-331-2882137

G. S. Tipenko
Geophysical Institute, University of Alaska,
Fairbanks, AK, USA

Introduction

A brief description of East Siberia Arctic Shelf environmental condition

The shelf of the Laptev Sea and the western part of the East Siberian Sea possesses flat bathymetry, relatively low depths (rarely exceeding 100 m) and a width reaching almost 1,000 km (Fig. 1). In these regions, neotectonic movements are of predominantly descend-

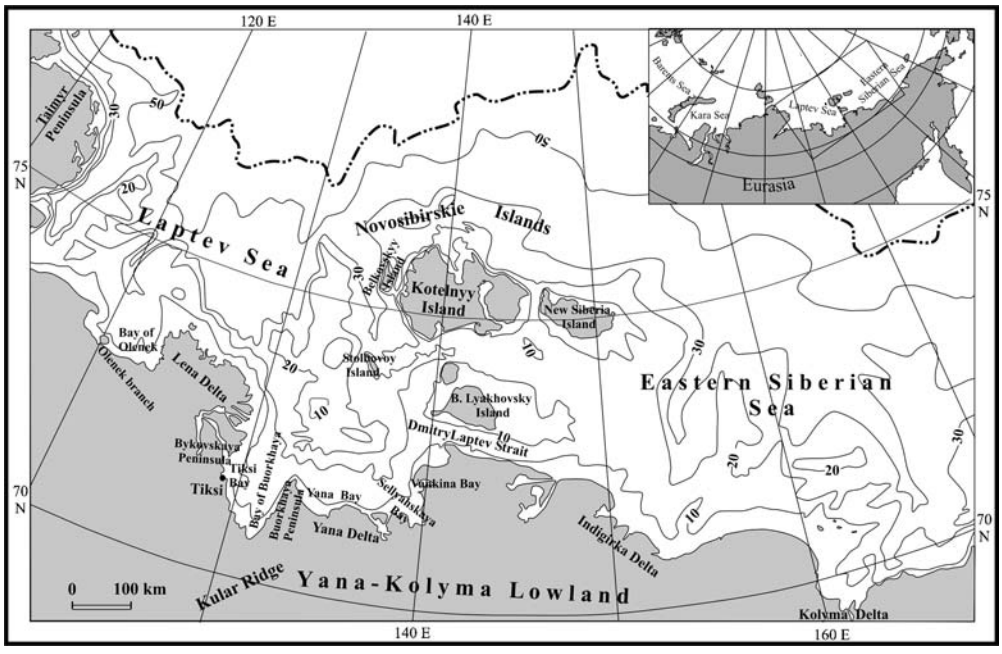

Fig. 1 Index map of the investigation area

ing character and accompanied by a compensatory accumulation of sediments. Until recently, it was believed that the East Siberian sector of the Arctic had not been subjected to major glaciations, at least during the Weaseling period. However, in the northeast of the region under study (in the northwestern part of the Novaya Sibir (New Siberian Island), Anisimov and Tumskoi (2003) have described massive ice beds that have some features that are indicative of glacial origin. These ice beds are covered by the Late Quaternary deposits of the ice complex (IC) or Yedoma formation. Thus, locally, in the northeastern part of the Novosibirskii Archipelago and adjacent shelf areas, the development of thin, local glaciers has taken place during at least one of the cold stages of the Late Cenozoic. However, over the larger part of this territory, glacial cover was absent. The geological and tectonic structure of this territory is extremely complicated; tectonic structures include both the Siberian Platform and the rift zone in the Laptev Sea, as well as many other minor structures (Drachev et al. 1995, 1999; Drachev 1998; Tectonic Map of the Kara and Laptev Seas and the North of Siberia 1998; Sekretov 1998, 1999; Franke et al. 1998, 2000, 2001). The continental part of these structures is characterized by considerable variations in the intensity of the geothermal heat flux, q_{gt}, which in the Moma and Baikal rifts can vary from 40 to 80 mW/m^2 within undisturbed blocks of the Earth crust, and exceed 100 mW/m^2 in fault zones (Balobaev 1991; Lysak 1988; Duchkov 1985; Duchkov and Sokolova 1985). It can be supposed that variations in the q_{gt} values within the shelf zone of the Laptev and East Siberian Seas are of the same magnitude. Heat-flow value data exist on Laptev Sea continental slope, with measurements ranging between 85 and 117 mWm^{-2}. A summary of heat-flow data in the Laptev Sea region and surrounding tectonic structures is shown in Fig. 7 of Drachev et al. (2003).

Our study of permafrost distribution and thickness in the shelf zone of Eastern Siberia is based on: (a) the result of works performed by Russian researchers before 1990s; (b) the results obtained within the framework of the joint Russian–German project entitled "Laptev Sea System" (Rachold and Grigoriev 1999, 2000, 2001; Rachold 2002; Grigoriev et al. 2003; Kassens et al. 1999; Pfeiffer et al. 2002); and (c) computer-based modeling, including the development of paleogeographic scenarios, geological models, and models of freezing–thawing of sediment-laden water.

The modeling was mainly based on the results of geological and geocryological surveys of the Novosibirskie Islands and coastal lowlands (the East Siberian shelf can be considered a continuation of this feature). These are the areas of continuous permafrost with a thickness from 300–400 to 500–600 m and more. Permafrost thickness data, though scarce, indicate that the depth of freezing is a function of permafrost temperature zonality as well as of the character of neotectonic structures. The latter differ from one another by the q_{gt} values and geological composition, including the thickness of unconsolidated Cenozoic deposits. Little observational data on the geology of shelf areas necessitates the use of hypothetical geological sections simplified for modeling purposes. The composition and properties of deposits and rocks in our models were selected in order to ensure that both maximum and minimum possible values for permafrost depth and thickness were obtained. Mean annual air temperature varies smoothly over the region under study, ranging from −13 to −15°C. The mean annual permafrost temperature (t_{ma}) ranges from −5 to −7°C in the southern part of the coastal lowlands (69°N–70°N) to −12 to −15°C in the

north (Novosibirskie Islands, 73°N–76°N), giving a mean latitudinal gradient of about 1.5°C/100 km.

The temperature of bottom seawater and sea surface sediments (t_{sf}) is equal (Zhigarev 1997). In the Laptev and East Siberian seas t_{sf} varies from −0.5 to −2.0°C (Dmitrenko et al. 2001). This favors the preservation of relic offshore permafrost because thawing from the top (i.e., from the sea bottom down) does not occur or occurs very slowly. An exception is observed near river mouths, where the seawater is freshened by the input of river water and has low, but above zero, temperature. In these areas, slow thawing of relic permafrost is possible. It is interesting that the thickness of the thawed layer increases with an increase in the seawater depth and with the age of shelf permafrost (submerging by freshened seawater) establishment under the sea. This can be illustrated by the results of drilling performed along a profile from the Bykovskaya Peninsula to the Mostakh Island in the Tiksi Bay with seawater freshened by the influence of the Lena River (A. Slagoda, personal communication). At the same time, formation of new permafrost is occurring on aggradational sedimentary features (bars, spits, barrier isles, etc.) in and around the river mouths (Grigor'ev 1966; Fartyshev 1993).

The general consensus is that the aggradation of permafrost within the East Siberian shelf occurred during the stages of the marine regression and shelf exposure. We support the idea about the glacioeustatic nature of transgression–regression cycles in the region, indicated by data on sea-level fluctuations in Eastern Siberian and Bering seas (Holmes and Creager 1974; Creager and McManus 1967; Hopkins 1976; Ivanov 1982; Veinbergs 1991; Selivanov 1996).

Formulation of the problem

The development of permafrost on coastal lowlands in northeastern Eurasia dates back to the Late Pliocene (Kaplina 1981; Sher 1984). Permafrost thawed in the warm climatic phases of the Pliocene–Pleistocene; first, fully, and then, only partially, from the top, so that the thickness of permafrost was only reduced. During cold phases, permafrost aggradation took place: the thickness of permafrost increased and its temperature decreased.

Up to the mid-1990s, little data were available that described the existence or nature of offshore permafrost. These data were generalized by Gavrilov et al. (2001). Most researchers believed that permafrost with relatively low thickness exists in the near-shore zone and is absent within the outer part of the shelf (Zhigarev 1981, 1997; Neizvestnov 1981; Solov'ev 1981). It was assumed that the degradation of relic permafrost proceeds mainly from the top, under the influence of warm seawater. The development of permafrost at the shelf was connected with the Late Pleistocene. According to Solov'ev (Solov'ev 1981; Solov'ev et al. 1987) and Neizvestnov (1981), offshore permafrost was formed after the Kazatsevskaya transgression (isotope stage 5e) and expanded considerably during the Sartan regression (isotope stage 2). However, Danilov (Danilov et al. 1997, 1998, 2000), Zhigarev (1981, 1997), and Fartyshev (1993) argued that permafrost initially formed later, during the Zyryanskii glacial period (isotope stage 4), degraded completely during the Karginskaya transgression (isotope stage 3), and appeared again in the Sartan cryochron and regression (isotope stage 2). According to these authors (except for Fartyshev 1993) the Sartan permafrost degraded considerably during the Holocene marine transgression (isotope stage 1).

More recently, large-scale studies of offshore permafrost in the Eastern Siberian Arctic have been conducted within the framework of joint Russian–German programs "Laptev Sea System" and "System Laptev Sea 2000." Results from these projects, together with earlier results obtained by Russian geologists, have been generalized in a number of papers (Romanovskii et al. 1997a, b, 1999, 2003; Kholodov et al. 1999; Romanovskii and Hubberten 2001a, b; Hubberten and Romanovskii 2000). In this paper, we perform the following: outline new data concerning the development of offshore permafrost on the eastern Siberian arctic sea shelf in relation to the problem of the gas hydrate stability zone (GHSZ); assess the potential thickness of this zone; and consider the evolution of the offshore permafrost and GHSZ under the impact of climate changes and glacioeustatic regression–transgression cycles. It should be noted that the problem of the presence and evolution of the GHSZ, in which natural gas exists in the form of metastable clathrate compounds (gas hydrates) as related to the evolution of permafrost, has not previously been considered, except by Delisle (1998). He modeled dynamic GHSZ during 160 ky before present for uniform ocean depth and a geothermal flux q_{gt} set to 60 mW/m^2. The variation of pressure caused by the submergence of the shelf over the time of transgression was not considered. In accordance with his modeling results, one or more GHSZ exists continuously on the Laptev Sea shelf. Permafrost and GHSZ prevents subpermafrost gas emission migration through the zone over the long-term.

Modeling approach to the problem of permafrost and GHSZ evolution within the shelf

Conditions and assumptions accepted in modeling of permafrost and GHSZ evolution within the shelf

The modeling approach to the reconstruction of permafrost evolution was previously proposed and described by Romanovskii and his colleagues for the shelf of Laptev Sea Region (Romanovskii et al. 1997a, b, 1998, 2003; Hubberten and Romanovskii 1999; Romanovskii and Hubberten 2001a, b). In this paper, the abovementioned modeling approach is applied to the shelf of

both seas, the Laptev and the East Siberian, and to the reconstruction of the evolution of GHSZ.

A paleogeographic scenario for the last 400,000 years has been established previously (Gavrilov et al. 2000, 2001; Romanovskii and Hubberten 2001a). The geological record of Middle Pleistocene and Holocene events in the coastal lowlands of Yakutia and Novosibirskie Islands is fragmentary; data on the age of particular strata are not very reliable (beyond the limits of radiocarbon dating). This circumstance makes it impossible to suggest a realistic paleogeographic scenario on the basis of exclusively regional data. The most suitable data on possible climatic fluctuations in many areas can be obtained from paleoclimatic curves based on the distribution of oxygen isotopes in ocean sediments and ice cores; it is also possible to use the curves based on the analysis of the contents of biogenic silica recovered from bottom sediments of Lake Baikal (Kuzmin et al. 2001). These are continuous curves reflecting climate fluctuations that operate at the largest scales, that is, those related to orbital parameters and having characteristic times of 100,000, 42,000, and 23,000–17,000 years.

A paleogeographic scenario for the Middle Pleistocene–Holocene interval in the studied region has been developed by us on the basis of a synthesis of regional data and an isotopic temperature curve from the Vostok ice core, Eastern Antarctica (Petit et al. 1999). The latter curve was used to provide an indication of global climate fluctuations. Paleotemperature reconstructions for the coastal lowlands of Yakutia were used as a regional data reference. These reconstructions were made by various researchers for reliably dated peaks of the most significant cold and warm stages. As a result, we have obtained regional paleotemperature curves reflecting deviations of permafrost temperatures from their modern values ($-t_{ma}$) for the East Siberian arctic shelf and coastal lowlands over the last 400,000 years (Gavrilov et al. 2000, 2001; Romanovskii and Hubberten 2001a, b). Climate fluctuations were accompanied by corresponding changes in the landscape and the character of the snow cover with corresponding effects on soil and permafrost temperatures. The most significant alterations of landscapes and snow cover (as compared with the modern epoch) took place during cold climatic states in the zone currently dominated by sparse forests and in the zone of arctic tundra and deserts. Therefore, separate paleotemperature curves have been developed for these zones.

The assumptions in the paleogeographic scenario

Several assumptions were made in the paleogeographic scenario used to set upper boundary conditions for the permafrost and GHSZ evolution model. First, it was assumed that the zonality pattern of t_{ma} in the past corresponded to the modern zonality of permafrost temperatures. The relief of the shelf zone in the past was considered to be the same as at present. The temperature of near-bottom seawater (equal to the temperature of the surface layer of shelf sediments (t_{sf}) (Zhigarev 1997) during transgression stages was set at −1.8°C; the freezing temperature of marine sediments or continental sediments saturated with seawater was assumed to occur at −2°C. This results in the position of the lower boundary of ice-bearing permafrost not being coincident with the 0°C isotherm. These mean that a permanent zone of cryotic deposits is located below ice-bearing permafrost with temperature −2°C and isotherm 0°C.

A series of curves indicating t_{ma} and t_{sf} variation by water depth were developed for the range of latitudes from 70°N to 78°N according to a procedure described earlier (Romanovskii et al. 1997a). Sea-level fluctuations were assumed to be of glacioeustatic nature. Several glacioeustatic curves, developed for particular time stages, were adapted for modeling purposes: from 400,000 to 120,000 BP, according to Petit et al. (1999); from 120,000 to 20,000 BP, according to Chappel et al. (1996); and from 20,000 BP to the present time, according to Fairbanks (1989). The latter curve (Fairbanks 1989) correlates well with observational data concerning Laptev Sea sea-level oscillations. These data were obtained during bottom sediment studies for the interval 11,000–9,000 BP (Bauch et al. 2001). It was assumed that permafrost temperature t_{ma} in any place changes to t_{sf} (−1.8°C) after submergence; land emergence is followed by a rapid change of permafrost temperature from −1.8°C to the t_{ma} typical of terrestrial permafrost at the corresponding latitude and time (Romanovskii et al. 1997a, 1998). It should be noted that the reliability of paleotemperature reconstructions is greater for the Late Pleistocene and Holocene than for the earlier epochs.

The initial conditions prescribed for the model assumed that there had been no ice-bearing permafrost on the shelf 400,000 years ago and that the temperature distribution in the vertical sections corresponded to normal temperature gradients. Our calculations were performed for different geological sections and different values of the geothermal flux q_{gt} (from 45 to 70 mW/m^2). These values of q_{gt} are typical for undisturbed blocks of earth crust in rift zones. One of the modeled geological sections, composed of unconsolidated Cenozoic deposits, characterized the situation in tectonic depressions. The presence of thick (up to 600 m) Cenozoic deposits is known from data recovered from a number of geophysical and borehole sites, including the lower reaches of the Kolyma River, the foothills of Kular Ridge, the Yana River delta, and the Buorkhaya Peninsula. Similar or even greater thicknesses of unconsolidated Cenozoic deposits is supposed for the rift zone in the Laptev Sea, judging from geophysical data (Sekretov 1998, 1999; Hinz et al. 1998 and other). These deposits are characterized by large porosity values and high water contents. This allows us to consider the modeled depth of their freezing at the geothermal flux value of 70 mW/m^2 as the minimum possible value

(Fig. 2a, b). The second modeled geological section is composed of hard rocks of the Verkhoyansk complex. Thermophysical properties of these deposits and rocks are given in Tables 1 and 2. The depth of freezing obtained for these deposits and rocks at the geothermal flux value of 45 mW/m^2 can be considered to represent the maximum possible value (Figs. 2a, 3a).

Modeling of the GHSZ evolution

The modeling of GHSZ dynamics was performed according to the model and corresponding software program developed by Tipenko et al. (1999). According to this model, the pressure (P) of groundwater at any depth is equal to the hydrostatic pressure of groundwater at that depth. The transgression of the sea generates additional pressure (ΔP) equal to the seawater pressure at the bottom of the sea, which transmitted in subpermafrost groundwater via open taliks. Thus, the hydrostatic pressure of groundwater increases by ΔP during marine transgressions and decreases during marine regressions. The pressure in aquifers below the relic permafrost is also equal to the hydrostatic pressure. In nature, this condition is ensured by the presence of open subsea taliks in active fault zones, under the channels of the largest rivers, and on the continental slope. While modeling the GHSZ, we used the curve of hydrate formation derived by Chuvilin and Perlova for porous media and methane and kindly submitted to us

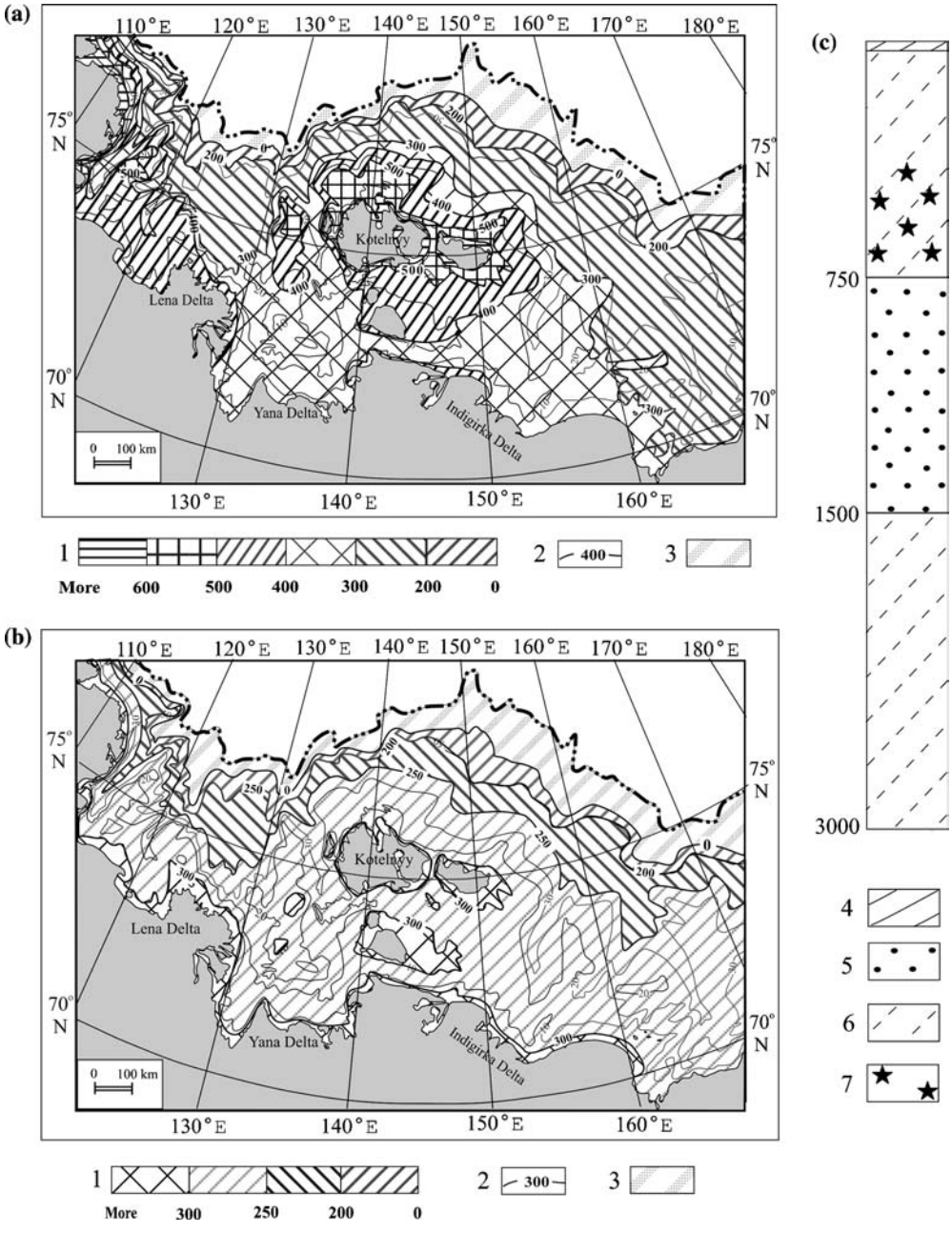

Fig. 2 Schematic map showing offshore permafrost thickness (results of simulation) for the "unconsolidated Quaternary deposits" geological regime. Geothermal heat fluxes (q_{gt}): **a** $q_{gt} = 45$ mW/m^2; **b** $q_{gt} = 70$ mW/m^2; **c** geological section: *1* ice bearing permafrost thickness, (m); *2* lines of equal permafrost thickness, (m); *3* outer zone of the shelf with discontinuous and island offshore permafrost; *4* marine silt; *5* fine sand; *6* loam; *7* gas hydrate inclusions

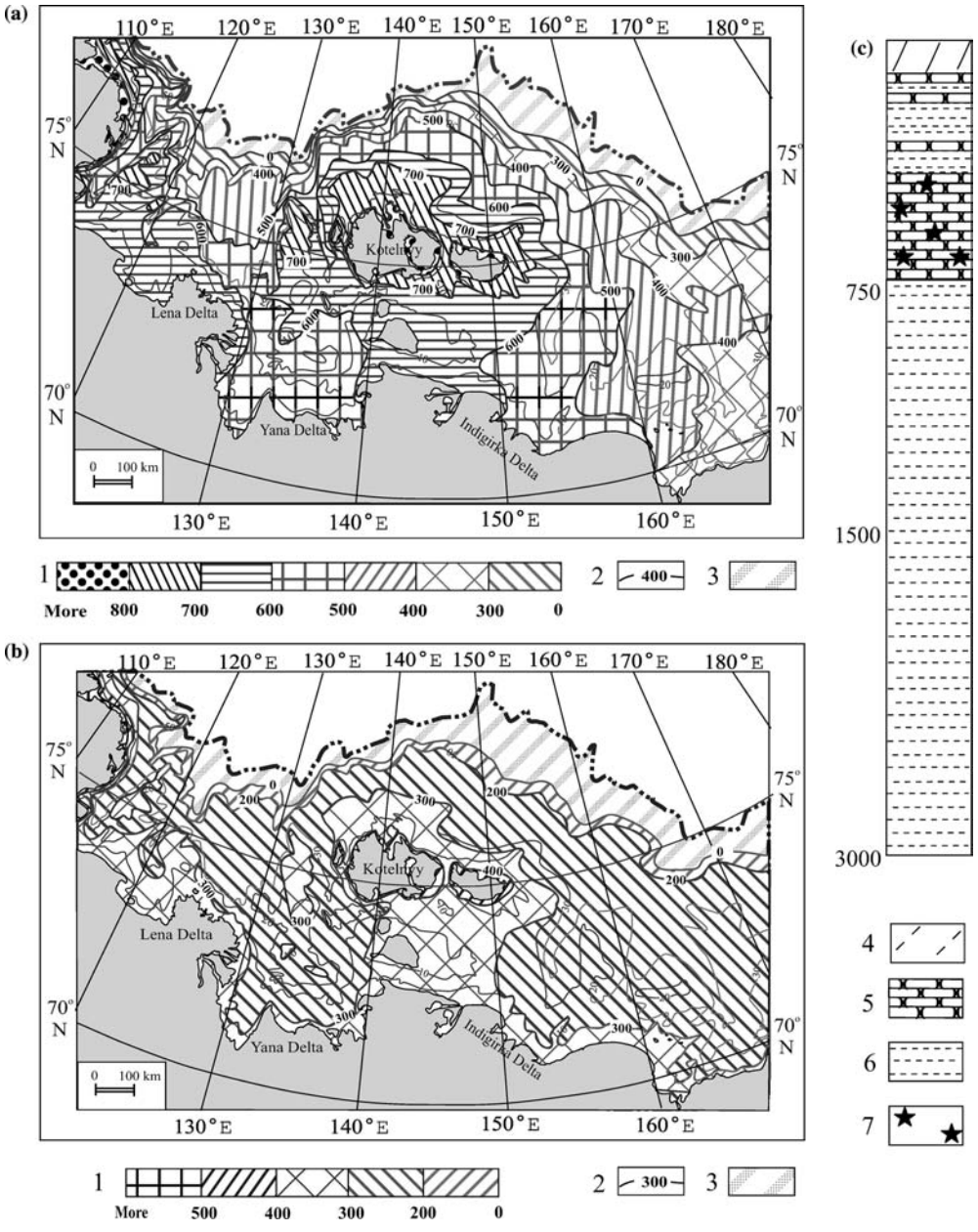

Fig. 3 Schematic map showing offshore permafrost thickness (results of simulation) for the ''consolidated bedrock'' geological regime. Geothermal heat fluxes (q_{gt}): **a** $q_{gt} = 45$ mW/m^2; **b** $q_{gt} = 70$ mW/m^2; **c** geological section: *1* ice bearing permafrost thickness, (m); *2* lines of equal permafrost thickness, (m); *3* outer zone of the shelf with discontinuous and island offshore permafrost; *4* marine silt; *5* sandstone; *6* argillite; *7* gas hydrate inclusions

by the authors (Chuvilin et al. 2000). The effect of groundwater salinity on the GHSZ was not taken into account because calculations were of approximate character. The evolution of the GHSZ was modeled using q_{gt} values of 45 and 70 mW/m^2, as indicated above. There is indirect evidence for the fact that these values are also typical of undisturbed blocks of the Earth crust within the shelf zone of both studied seas. On the basis of our calculations, schematic maps of the position of the lower boundary of the GHSZ at the present time were compiled (Figs. 4, 5). These maps, as well as maps of relic offshore permafrost thickness, reflect the presence of the GHSZ and the lower depth of its boundary for tectonically undisturbed blocks of the earth's crust. They do not take into account geothermal anomalies in active fault zones. Along with the maps, the results of our calculations are presented using plots reflecting changes in the temperature field, permafrost thickness, and the lower boundary of the GHSZ for different time intervals. These plots were developed for different latitudes and different ocean depths. An example of corresponding calculations is shown in Fig. 8. The upper boundary of the GHSZ obtained during our modeling lies within the permafrost where changes in hydrostatic pressure due to marine regressions and transgressions cannot reach due to the absence of free water in pore media, which is filled by ground ice and hydrate. Therefore, this represents a so-called ''conventional'' boundary that reflects the upper position of the GHSZ at the beginning of permafrost formation on the shelf and/or possible position of hydrate in pore ice.

Table 1 Deposit property parameters used in the model for geological section 1

Layers thickness (m)	Deposits	Heat capacity (J/m^3 K)		Thermal conductivity λ (W/mK)		Moisture, W (%)	Latent heat[c] (J/m^3 K)
		Thawed, C_{th}	Frozen, C_{fr}	Thawed, λ_{th}	Frozen, λ_{fr}		
10	Heavy loam[a]	1.7×10^6	1.4×10^6	1.16	1.84	27.24	114.5×10^6
740	Sand, loam[a]	1.1×10^6	0.8×10^6	1.26	1.46	22.46	114×10^6
750	Sand[a]	1.0×10^6	0.9×10^6	1.15	1.17	5.09	94×10^6
1,500	Sand, loam[a]	1.1×10^6	0.9×10^6	1.82	2.43	22.46	124×10^6
200	Gas hydrate in sand and loam deposits[b]	1.1×10^6	0.8×10^6	1.26	0.44	22.46	122×10^6

[a]Thermophysical properties in accordance with Balobaev (1991)
[b]Thermophysical properties in accordance with Groisman (1985)
[c]Glossary of Permafrost and Related Ground-Ice Terms (1988)

Table 2 Bedrock property parameters used in the model for geological section 2

Layers thickness (m)	Bedrock	Heat capacity (J/m^3 K)		Thermal conductivity λ (W/mK)		Moisture, W (%)	Latent heat[c] (J/m^3 K)
		Thawed, C_{th}	Frozen, C_{fr}	Thawed, λ_{th}	Frozen, λ_{fr}		
100	Salty loam[a] $D_s = 1.0\%$	1.13×10^6	0.86×10^6	1.37	1.91	17.47	114.5×10^6
20	Sandstone[a]	0.8×10^6	0.78×10^6	1.14	1.17	3.01	94×10^6
20	Argillite[a]	0.88×10^6	0.85×10^6	1.43	1.45	3.25	104×10^6
20	Sandstone[a]	0.81×10^6	0.79×10^6	1.23	1.26	3.57	94×10^6
90	Argillite[a]	0.87×10^6	0.84×10^6	1.44	1.47	3.84	108×10^6
50	Sandstone[a]	0.81×10^6	0.79×10^6	1.33	1.37	4.67	96×10^6
50	Argillite[a]	0.86×10^6	0.83×10^6	1.48	1.52	5.01	112×10^6
400	Sandstone[a]	0.82×10^6	0.81×10^6	1.49	1.53	5	98×10^6
2250	Argillite[a]	0.89×10^6	0.88×10^6	1.51	1.54	5.12	125×10^6
200	Gas hydrate in sandstone deposits[b]	0.82×10^6	0.81×10^6	1.49	0.46	5	98×10^6

[a]Thermophysical properties in accordance with Balobaev (1991)
[b]Thermophysical properties in accordance with Groisman (1985)
[b]Glossary of Permafrost and Related Ground-Ice Terms (1988)

Comparison of modeling to field data

The analysis of the simulation results shows that the current distribution and thickness of relic offshore permafrost (Figs. 2a, b and 3a, b) depends on the three groups of factor. The first group is related to the tectonic position of a particular plot, which dictates the intensity of geothermal flux q_{gt} and the composition and thickness of unconsolidated Cenozoic deposits. The second group is related to the depth of the sea, which specifies the duration of freezing during regression stages and the duration of offshore permafrost submergence during transgression stages. The third group is associated with the latitudinal zonality of terrestrial mean annual ground permafrost temperature t_{ma} (°C), which controls the depth of freezing during regression stages. In agreement with these factors, the greatest thickness of offshore permafrost at the present time is predicted for the nearshore zone in the western part of the Laptev Sea. This part of the shelf belongs to the Siberian Platform (Tectonic Map of the Kara and Laptev Seas and the North of Siberia 1998; Duchkov 1985; Balobaev 1991; Drachev et al. 2003) and is characterized by low $\mathbf{q}_{gt}$ values. The latter is confirmed by the low values of the geothermal gradient measured in the areas of Kozhevnikova Bay and Uryung-Tumus Peninsula for depths ranging from 200 to 500 m (1.4–0.4°C/100 m). These starting values return offshore permafrost depth estimates in the range of 600–800 m, according to Ponomarev (1937, 1960). Fartyshev (1993) has calculated the thickness of offshore permafrost in these areas in the range 1,000–1,300 m. Similar values were predicted for the Olenek branch in the Lena Delta. If the calculations are based not on the average value of the geothermal gradient in borehole no. 5 (the Chai-Tumus key plot), which was made by Grigor'ev (1966), but instead on the values typical of the lower measured section (230–330 m), then the thickness of permafrost should be up to 800–1,100 m. Taking this into account, we can state that the modeled thickness of offshore permafrost equal to 600–700 m for a section composed of consolidated bedrocks at q_{gt} = 45 mW/m^2 (Fig. 3a) is close to the values typical of coastal shoals in the western part of the Laptev Sea.

A considerable thickness of permafrost is predicted for the areas around the Novosibirskie islands. This is governed by the position of these shallow-water areas in high latitudes, where the duration of shelf exposure during marine regressions and associated drying of the

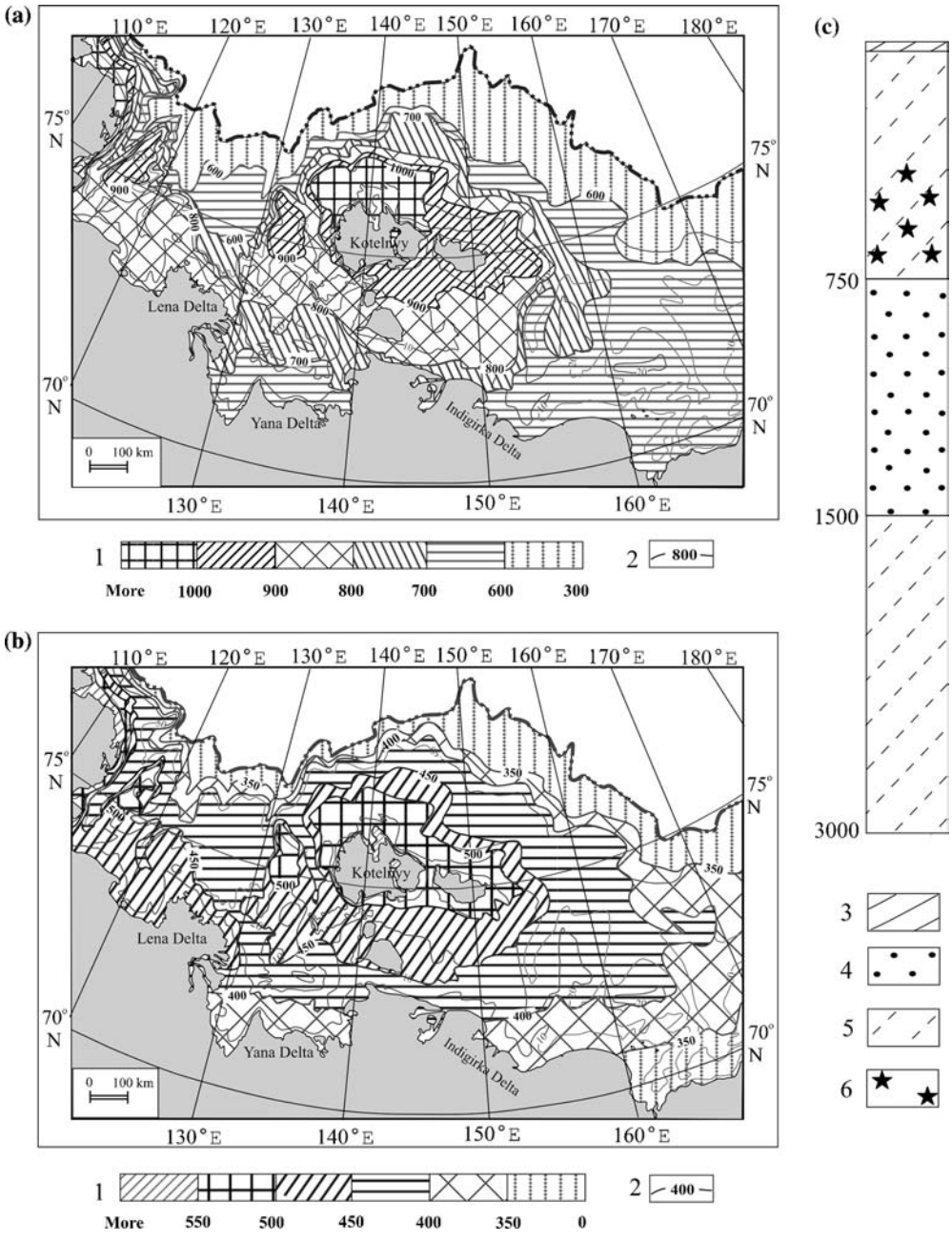

Fig. 4 Schematic map showing the lower boundary position of the gas hydrate stability zone; simulation results for the ''unconsolidated Quaternary deposits'' geological regime. Geothermal heat fluxes (q_{gt}): **a** $q_{gt} = 45$ mW/m^2; **b** $q_{gt} = 70$ mW/m^2; **c** geological section of Quaternary deposits: *1* position of GHSZ lower boundary (distance from a sea floor), (m); *2* lines of equal position of lower boundary of GHSZ, (m); *3* marine silt; *4* fine sand; *5* loam; *6* gas hydrate inclusions

shelf and penetration of frost into the rocks was greatest, and by the fact that the duration in the submerged state during the last transgression was shortest. The 2-D surveys carried out by the German/Russian cooperative expedition (BGR, Germany and Russian institution SMNG, Murmansk) revealed northward from Kotel'ny Island the existence of 300–800 m thick seismic sequences beneath the sea floor, characterized by a distinct high-reflective and mostly subparallel pattern. These distinct sequence crosscuts and masks represent real structural features. For this reason, the distinct superficial seismic sequence was interpreted as a permafrost layer (Hinz et al. 1998). An explanation for the wide variance in permafrost thicknesses observed in this region, given by Delisle (1998), relates to a combination of uneven sea depth, different q_{gt} values, different geological construction, and varying thermophysical properties of rocks and deposits in the various tectonic elements present on the shelf. The variation of the condition of the sea floor environment, mentioned above, is probably greater than accounted for our modeling data.

Thus this region is characterized by generally high but unevenly distributed geothermal flux values q_{gt}. Geothermal measurements in boreholes on Novosibirskie Islands demonstrated the existence of low mean annual ground temperatures (−13 to −15°C) and steep geothermal gradients (up to 5–6°C/100 m), (Solov'ev et al. 1987). It can be supposed that these boreholes were drilled in the active tectonic zone. Unfortunately, these data are scarce and there are virtually no temperature

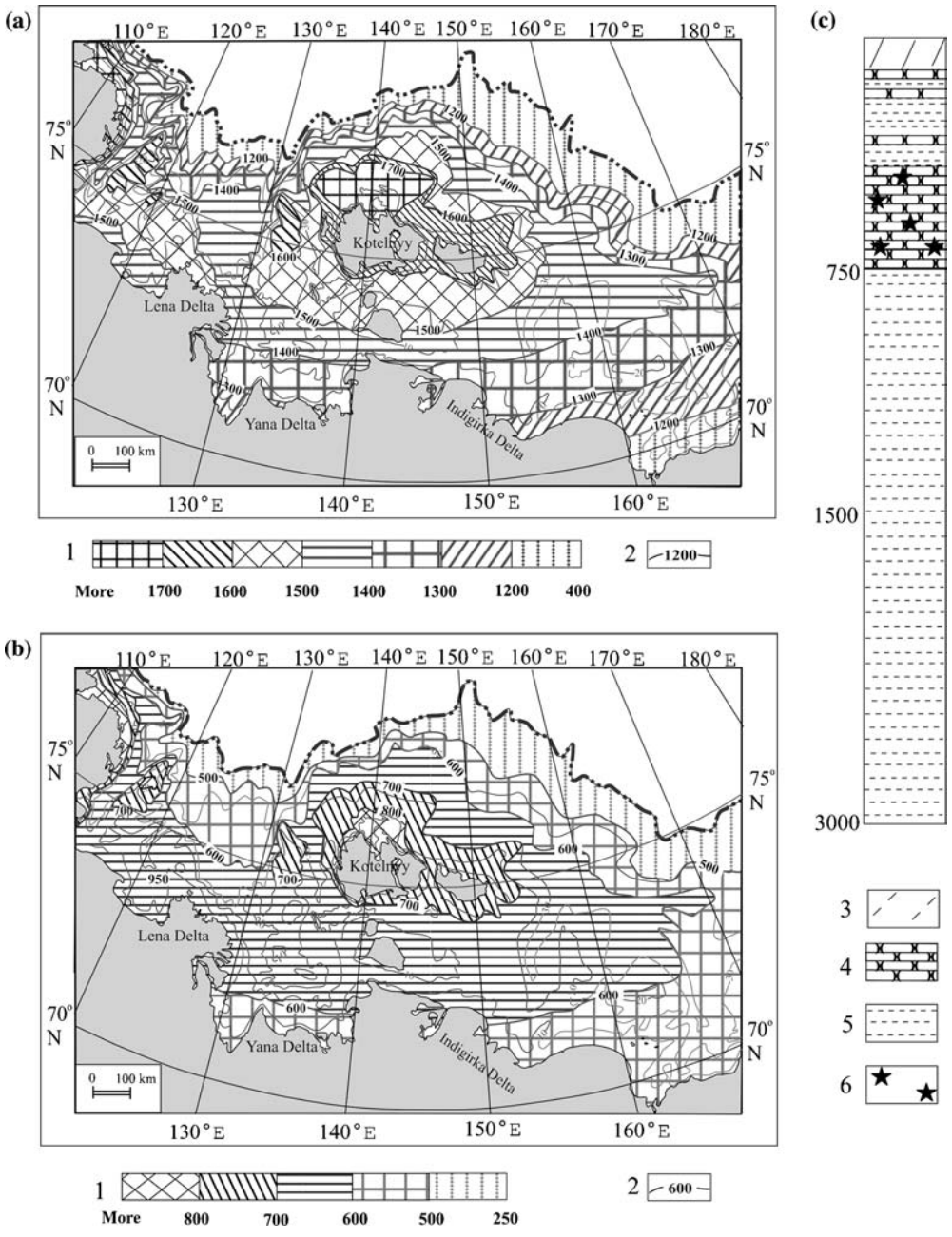

Fig. 5 Schematic map showing the lower boundary position of the gas hydrate stability zone; simulation results for the ''consolidated bedrock'' geological regime. Geothermal heat fluxes (q_{gt}): **a** q_{gt} = 45 mW/m^2; **b** q_{gt} = 70 mW/m^2; **c** geological section: *1* position of GHSZ lower boundary (distance from a sea floor), (m); *2* lines of equal position of lower boundary of GHSZ, (m); *3* marine silt; *4* sandstone; *5* argillite; *6* gas hydrate inclusions

measurements below 200 m. The calculated values of geothermal gradients correspond to gradients typical of rift zones (3–6°C/100 m and even higher); the intensity of geothermal flux in such zones, according to the Geothermal Map of the World (1988) is 50–100 mW/m^2 and higher. Geothermal flux measurements on the continental slope close to the connection of Gakkel Ridge and its shelf continuation, proposed by Drachev et al. (2003), supported the idea that the rift zones on the shelf possibility have large values of q_{gt}.

It is probable that the values of permafrost thickness displayed in Fig. 3b (500–600 m) are near the maximum possible values for the area of the Novosibirskie Islands. The analysis of the shelf zone modeling results, as well as data from high-frequency acoustic soundings and geothermal observations in boreholes on the Novosibirskie Islands, allow a refinement of offshore permafrost thickness estimates to 400–450 m to be made. In the zones of tectonic faults, as evidenced by geothermal data obtained on the islands (Solov'ev et al. 1987; Neizvestov et al. 1976), this thickness may be further reduced to 200–250 m.

The thickness of offshore permafrost in near-shore, shallow-water areas within the eastern part of the Laptev Sea and the western part of East Siberian Sea varies considerably, depending on neotectonic conditions. For instance, in Yana Bay, the predicted values vary from 400–300 m (Fig. 2a) in tectonic uplifts, to 300–250 m (Fig. 2b) in active rift zones composed of a thick layer of unconsolidated Cenozoic sediments. This can be as-

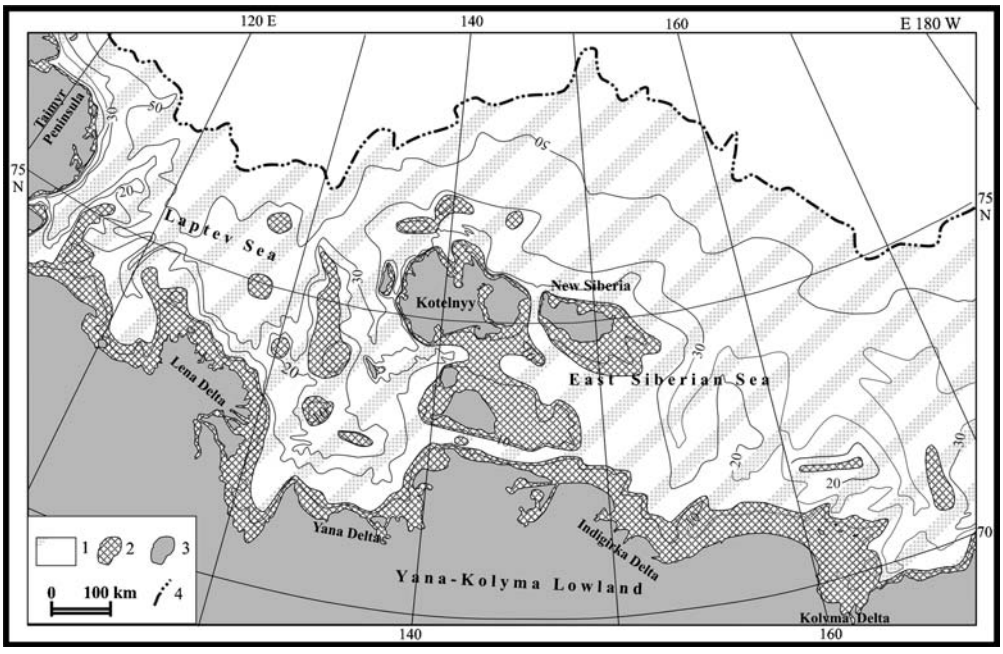

Fig. 6 Schematic map showing permafrost state: *1* ice bearing offshore permafrost: *2* ice bonded offshore permafrost; *3* terrestrial ice bonded permafrost; *4* boundary of the Arctic Shelf

sumed from data on the permafrost thickness in coastal areas: 620 m in bedrock near the settlement of Tiksi (Grigor'ev 1966; Devyatkin 1993) and 350–470 m of unconsolidated sediments in the Yana Delta (data from borehole drilling for the purposes of water supply). In a grabben at the foothills of the Kular Ridge, the thickness of permafrost may reach 700 m, as estimated from borehole temperature measurements for the upper 400 m (Khrutskii et al. 1977).

A schematic map of offshore relic permafrost state (Fig. 6), compiled on the basis of modeling results and field observations, shows the distribution of relic ice-bearing and ice-bonded permafrost on the Arctic shelf. Rift areas, where the thickness of permafrost varies considerably and the occurrence of deep, open taliks is possible along the active faults, are identified on the map in Fig. 7.

Discussion

Modeling assessment

The modeling of permafrost dynamics was performed using for an initial condition the complete absence of permafrost within the shelf 400,000 years ago (Fig. 8). As seen from Fig. 8, the offshore permafrost thickness dynamics is conditioned by the alternation of regres-

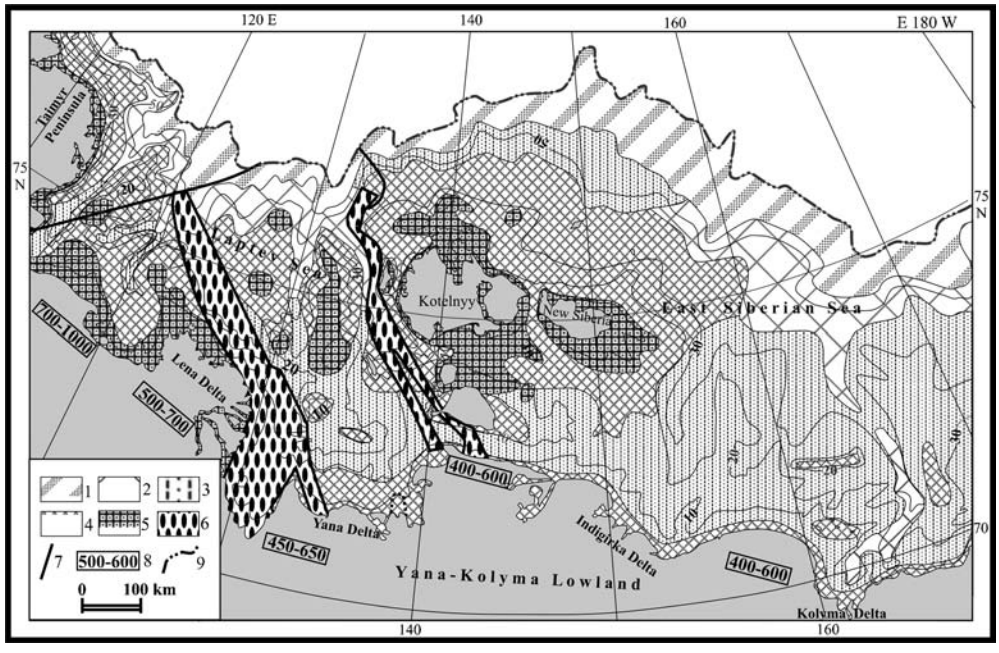

Fig. 7 Schematic map showing relic offshore ice bearing permafrost thickness on the East Siberia Arctic Shelf (Simulation results using a geothermal heat flux of 45 mW/m^2). Ice bearing permafrost thickness, (m): *1* discontinuous, ≤ 100; continuous *2* 100–200; *3* 200–300; *4* 300–400; *5* 400–600; *6* 100–600 in rifts with open taliks; *7* open taliks following large tectonic fractures (supposed); *8* coastal permafrost thickness; *9* Arctic Shelf boundary

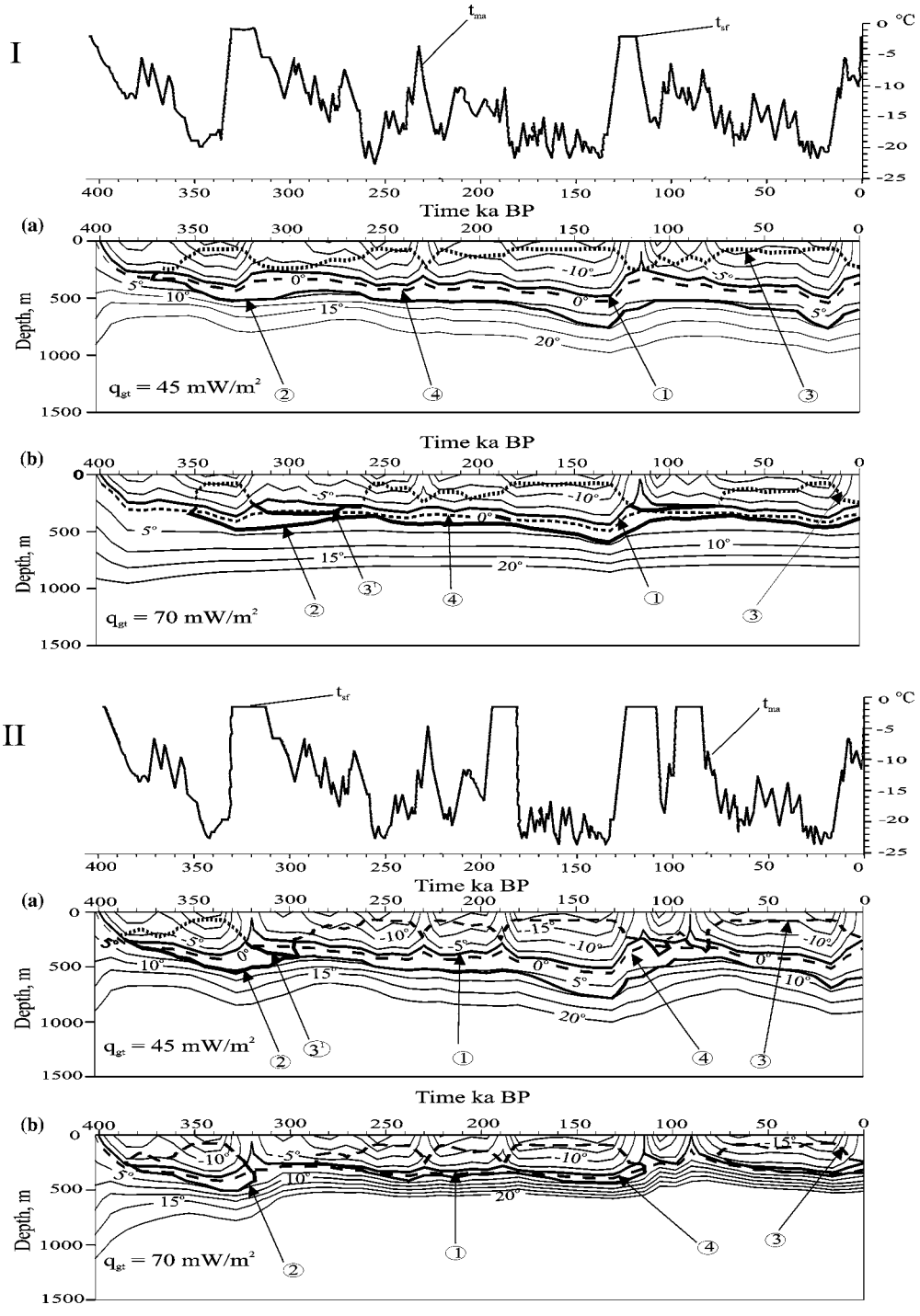

Fig. 8 Evolution of offshore permafrost thickness and GHSZ position during 400,000 years (*lower panel*): *I* for latitude 70° N with recent seawater depth 10 m; *II* for latitude 71°N with recent seawater depth 30 m. Geothermal heat fluxes (q_{gt}): **a** q_{gt} = 45 mW/m^2; **b** q_{gt} = 70 mW/m^2. The *circled numbers* on the graphs are as follows: *1* a lower border of ice bearing permafrost (temperature −2°C); *2* lower border of GHSZ; *3* upper border of GHSZ inside of ice bearing permafrost is shown conditionally; 3^1 upper border of GHSZ below of lower border of ice bearing permafrost; *4* isotherm 0°C. Upper panel: variation of mean annual ground temperature t_{ma} on emergent shelf and sea floor temperature t_{sf} during transgression periods

sion and transgression stages and, hence, corresponding changes in the t_{ma} and t_{sf} values. The amplitude of changes in the thickness of permafrost is greater for the blocks possessing large geothermal flux values, q_{gt} = 70 mW/m^2, than for the blocks with q_{gt} = 45 mW/m^2. The total thickness of permafrost is higher than the thickness of ice-bearing permafrost, because of the presence of the zone of cryotic deposits with unfrozen saline water below the ice-bearing permafrost. The total thickness of permafrost, as well as the thickness of ice-bearing permafrost, is reduced during transgressions. However, this reduction is more pronounced for ice-bearing permafrost than for the total thickness of permafrost. Therefore, the overall thickness of the zone with cryotic deposits increases during the transgressions (Fig. 8). This is especially true for areas with considerable water depths. In these areas, within the blocks having q_{gt} = 70 mW/m^2, ice-bearing permafrost might degrade completely towards the end of transgression stages, so that permafrost is only represented

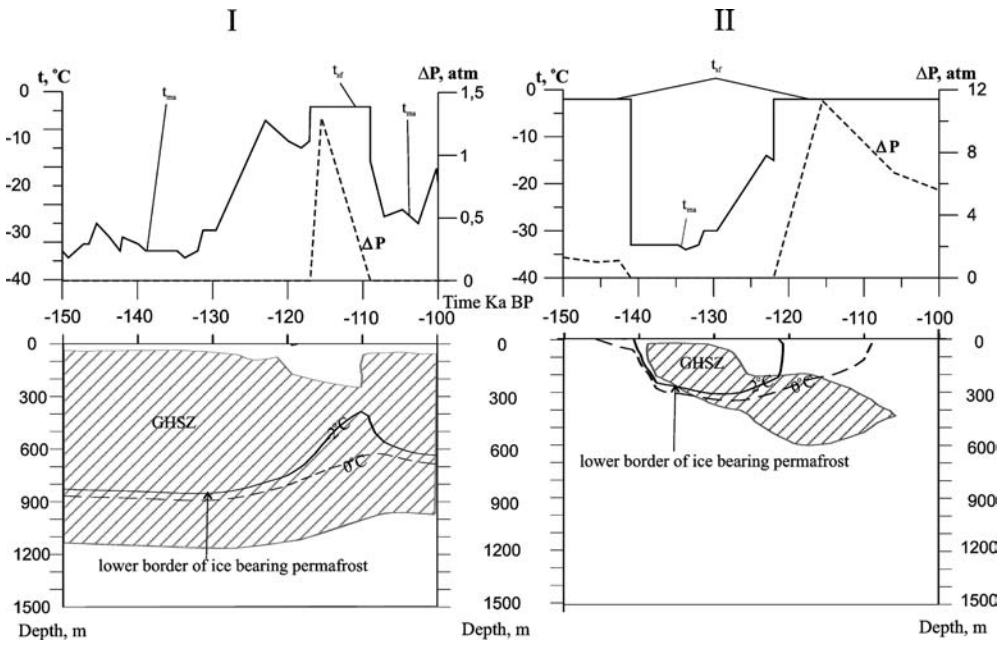

Fig. 9 Evolution of ice bearing permafrost thickness and GHSZ position on the shelf (*upper panel*); *I* geothermal heat flux $q_{gt} = 45$ mW/m^2; seawater depth 20 m, latitude 72° N; *II* geothermal heat flux $q_{gt} = 70$ mW/m^2 seawater depth 100 m, latitude 77° N (*lower panel*); On upper panel: variation of mean annual ground temperature (t_{ma}) and/or sea floor temperature (t_{sf}) (*solid line*) and excess pressure (ΔP)

by cryotic sediments (Figs. 9-II, 2a, b and 3a, b). At present, i.e., at the final stage of the Late Pleistocene–Holocene transgression of the sea, perennially frozen rocks still exist at considerable depths in lithospheric blocks composed of hard rocks and subjected to geothermal flux of up to 45 mW/m^2 (Fig. 2a). This is in contrast to blocks with geothermal flux of 70 mW/m^2, which have thawed out. Thus, in the outer shelf zone (with sea depths >60 m), ice-bearing permafrost should have a discontinuous or sporadic distribution. (Fig. 3a, b).

Model values of the thickness of permafrost decrease to the east of the Novisibirskie Islands, which is conditioned by the more southerly position of the modern coastline and the outer edge of the shelf.

The evolution of permafrost under the impact of climate change and transgression–regression cycles on the shelf and in coastal lowlands is characterized by a time lag. (Figs. 8, 9). During warm stages and marine transgressions, the maximum thawing of permafrost from the top and the minimum thickness of permafrost are achieved much later than corresponding climatic peaks; the greater the seawater depth, the greater the time lag (Figs. 8, 5) (Some numbers are in the following examples). Thus, for the Kazantsevskaya transgression (isotope stage 5e), this lag is equal to 35–40 ka for a depth of about 30 m (Fig. 8-II), and to 7 ka for a depth of about 10 m. Thus, the minimum thickness of relic permafrost on the shelf is observed at the beginning of the next stage of its drying (in the given example, it corresponds to the cooling phase in the Late Kazantsevskoe time). For depths of about 10 m, this happened 117 ka BP (Fig. 8-I); for depths of 30 m, about 90–83 ka BP. Similarly, during cold stages and sea regressions, the maximum thickness of permafrost is achieved later than the time of climatic minimums.

Calculations show that maximum values of permafrost thickness in the end of corresponding aggradation stages are proportional to the values of the geothermal flux q_{gt}, provided that all other factors are similar. The rates of permafrost aggradation decrease by the end of aggradation stages. In contrast, during periods of climate warming and marine transgressions, which are accompanied by increasing mean annual permafrost temperature t_{ma} and the surface layer of bottom sediments temperature t_{sf}, the rate of permafrost thawing from the bottom first increases and then, after the transformation of the temperature field of permafrost into the gradient-less field, becomes constant. The rate of permafrost thawing from the bottom increases with an increase in q_{gt} values, provided that all other factors are similar. Thus, during warming stages, the thickness of permafrost within the shelf and coastal lowlands decreases due to thawing from the bottom under the impact of geothermal flux. This is accompanied by a differentiation of permafrost thickness values among different lithospheric block units possessing different q_{gt}. Taking into account the time lag effect, maximum differences are observed at the beginning of cooling stages on coastal lowlands and during the final stages of marine transgressions on the shelf.

As demonstrated in the simulation, alterations of the permafrost temperature regime within the shelf during marine transgressions proceed in two stages. In the first stage, after the flooding of the shelf by seawater and a rapid growth of the temperature at the surface of relic permafrost from t_{ma} to t_{sf} (−2°C), a gradual leveling of temperatures from the offshore permafrost table to its bottom takes place; this is accompanied by the transformation of ice-bonded permafrost into ice-bearing permafrost with zero temperature gradients. The thawing rate of ice-bearing permafrost gradually increases. In

the second stage, the thawing of ice-bearing permafrost proceeds at a constant rate, depending on the value of geothermal flux q_{gt}, thermophysical properties of frozen rocks, and their ice content.

Analysis of model results also shows that massifs of ice-bonded permafrost should be preserved within nearshore, shallow-water areas and shoals, as well as in places of vanishing islands that are composed of ice complex sediments (Gavrilov et al. 2003). The temperature of the latter is below the freezing–thawing range of temperatures for clayey sediments saturated with saline seawater. At greater water depths, the permafrost thickness is reduced due to its long-term thawing from the bottom. The temperature field in the deposits has zero gradients, and the temperature of these deposits is near the thawing–freezing point. This kind of permafrost is referred to as ice-bearing permafrost. Ice-bonded and ice-bearing permafrost have different physical-mechanical properties, which hampers understanding of their nature. Thus, ice-bearing permafrost is characterized by low velocities of seismic waves, which makes it rather close to unfrozen rocks. We have developed a map showing the distribution of ice-bonded and ice-bearing permafrost within the shelf according to the modeling results (Fig. 8). As seen from this map, the largest part of the shelf is occupied by ice-bearing permafrost (Hubberten and Romanovskii 2003).

The map of the thicknesses of permafrost and GHSZ, as based on model calculations using q_{gt} values equal to 70 mW/m^2 (Figs. 2b, 3b, 4b, and 5b), shows that within the outer part of the shelf with recent water depths of about 60 m, permafrost is absent, whereas the GHSZ is present. The upper boundary of the latter should lie at a depth of about 200 m below the sea bottom. The thickness of the GHSZ is relatively low and does not exceed several hundred meters. At the further rise in sea level, the GHSZ should be preserved; at a decrease in sea level, it should be reduced owing to a decrease in ΔP values.

Our modeling of the dynamics of permafrost and GHSZ encompasses a period of 400 ka and assumes the absence of permafrost and GHSZ in the beginning of this period. The formation and development of permafrost during regression stages and drying of the shelf have been accompanied by the appearance of the GHSZ. According to the results of modeling, the upper boundary of the GHSZ should lie within the permafrost thickness. It should be stressed that this boundary has a "conventional" character, because changing of additional hydrostatic pressure (ΔP) in sub-permafrost water cannot be transmitted in the permafrost. This boundary is shown by dashed lines on corresponding plots (Fig. 8). At the same time, during transgression stages, the upper boundary of the GHSZ descends and becomes separated from the lower permafrost boundary. Therefore, on corresponding plots (Fig. 8), these events are marked by a special symbol (3^1). However, we do not know if this phenomenon, predicted by our model, really takes place under natural conditions. If it does, it should be accompanied by a migration of gases and their accumulation immediately below the frozen layer. Then, these gas accumulations may be transformed into gas hydrates. The complete disappearance of the GHSZ is predicted for long-term transgression stages in the areas with an increased geothermal flux (q_{gt}) (Fig. 9-II). The separation of the upper boundary of the GHSZ from the bottom of permafrost takes place under the same conditions.

The stability zone of the gas (methane) hydrates on coastal lowlands is formed simultaneously with the aggradation of permafrost up to 300–400 m and exists continuously during both warm and cold climatic periods. The lower boundary of the GHSZ within coastal lowlands is found about 300 m below the lower boundary of permafrost. The dynamics of the GHSZ in coastal lowlands follows the same pattern as the dynamics of permafrost with some time lag. It is entirely controlled by changes in the temperature of rocks, because hydrostatic pressure is assumed to be constant. The upper boundary of the GHSZ in coastal lowlands, as well as within the shelf, lies within the thickness of frozen rocks. At the point when a shelf is emerging due to regressions, the dynamics of the GHSZ and the thickness of permafrost within coastal lowlands and on the shelf is the same. During transgressions, this dynamic is different for the outer and inner parts of the shelf. In this time, on one hand, the temperature of rocks increases and the thickness of permafrost decreases; on the other hand, the excessive pressure ΔP increases because of the increase in the sea depth. An example (Fig. 9) illustrates the results of modeling for the time interval from 150 to 100 ka BP, made for the 20 and 100-m isobaths. In the inner shelf zone, both permafrost and the GHSZ continue to exist (Fig. 9-I). In the outer shelf zone, permafrost and the GHSZ degrade completely by the end of the transgression. At the same time, in the beginning of transgressions, permafrost is subjected to gradual degradation, whereas the GHSZ continues to exist or even enlarges (Fig. 9-II). This is conditioned by an increase in the water depth with a corresponding increase in hydrostatic pressure (ΔP). Judging from the results of modeling, at present, within lithospheric blocks with q_{gt} of 45 mW/m^2, the thawing of permafrost will come cease and a the GHSZ will continue to gradually increase in thickness in the vicinity of the 100-m isobath.

Within lithospheric blocks with q_{gt} of 40–50 mW/m^2, permafrost does not thaw out completely during transgression stages and exists as an impermeable screen for ground water and gases below the permafrost at sea depths up to 40–45 m. At greater depths and at greater q_{gt}, local or total thawing of permafrost takes place; the GHSZ can also disappear. These processes may lead to an increased emission of gases in the end of transgression stages.

Conclusions

1. The studies performed give additional evidence for the presence of ice-bearing and ice-bonded permafrost

and the GHSZ on the shelf of arctic seas in Eastern Siberia. A conclusion about the presence of permafrost within the entire shelf zone, up to its outer edge, has been made earlier for the Laptev Sea shelf (Romanovskii et al. 1997a, b). In this paper, we argue that the situation is similar for the East Siberian region, and in fact it is typical of the western part of the shelf in the East Siberian Sea. The greater part of the shelf, out to the 50 to 60-m isobath, is occupied by continuous ice-bearing and ice-bonded relic offshore permafrost. In deeper areas, for example close to the outer edge of the shelf, the distribution of ice-bearing and ice-bonded relic offshore permafrost has a discontinuous character. Ice-bearing and ice-bonded relic offshore permafrost is preserved in the areas with relatively low values of geothermal heat flux ($q_{gt} <$ 40–50 mW/m^2). In the remaining part of the shelf, the presence of cryotic deposits characterized by subzero temperatures and the absence of ice is predicted.

2. Within the greater part of the shelf, degrading, ice-bearing relic offshore permafrost predominates. The presence of relic ice-bonded offshore permafrost is presumed to exist at recently eroded islands composed of the Ice Complex deposits (at present, shoals and bars exist in place of these islands) and in the near-shore areas, where a retreat of the coasts destroyed by thermal erosion is observed.
3. Shoals in place of the former islands are subjected to active sea floor thermal erosion. As a result, sediments and organic substances from the degrading Ice Complex are released into the sea; this process is especially active in the lower horizons of the Ice Complex found below sea level. The scale of this process is very large and is observed over vast territories. The input of organic carbon into arctic seas due to the sea-floor thermal erosion is comparable with or even exceeds the input of organic carbon from coastal erosion and river discharge. Along with this, sea-floor thermal erosion and resuspension of thermal eroded sediments in seawater contribute to distant transfer, i.e., beyond the shelf zone, of fine fractions of mineral and organic matter. Most of the resuspended matter is from eroded Ice Complex deposits. At the same time, the accumulation of sandy material takes place close to the location of sea floor thermal and shore erosion. This phenomenon of particle-size fractionation of eroded sediments may be the reason for the widespread presence of sand in bottom sediments on the shelf of arctic seas in the Eastern Siberian sector of the Arctic.
4. The Arctic shelf of Eastern Siberia, along with the presence of ice-bearing and ice-bonded relic offshore permafrost, is characterized by favorable conditions for the preservation of a thick zone of stable gas hydrates. Permafrost and the gas hydrate stability zone prevent the emission of greenhouse gases from the layer underlying permafrost.
5. The modeling of the evolution of the thickness of ice-bearing and ice-bonded relic offshore permafrost and the zone of stable gas hydrates attests to the fact that both phenomena have continuously existed within the larger part of the shelf for at least four climatic and glacioeustatic cycles, i.e., at least for 400,000 years. Climate changes and transgression–regression cycles affect the thicknesses of permafrost and the evolution of the zone of stable gas hydrates because the upper and lower boundaries of GHSZ are subjected to some fluctuations.
6. The results of our investigations show that the evolution of ice-bearing and ice-bonded relic offshore permafrost and the GHSZ have both similarities and distinctions. In general, aggradation of permafrost is accompanied by the expansion of the GHSZ. The differences between the dynamics of permafrost and the GHSZ increase from the inner to the outer part of the shelf and are related to the following factors:

   (a) A decrease in the duration of permafrost aggradation stages and an increase in the duration of permafrost degradation stages from the inner to the outer part of the shelf
   (b) An increase in the effect of additional hydrostatic pressure caused by regressive–transgressive cycles in sea level in the same direction; and
   (c) Differences in the effect of the sea on the thickness and state, i.e., ice-bonded or ice-bearing, of relic offshore permafrost, on one hand, and the GHSZ, on the other hand.

   At present, in the peripheral part of the shelf, the degradation of the massifs and islands of ice-bearing relic offshore permafrost takes place. At the same time, the GHSZ is either stable or even increasing under the impact of rising sea level in the outer shelf zone.
7. The study of the current state of permafrost and the GSSZ as well as forecasts of future changes for different parts of the shelf should take into account regional differences. In this context, the evolution of these natural phenomena in the past acquires special significance. Thus, further investigations into the dynamics of these phenomena and their modeling and reconstruction are required.

Acknowledgements This study was supported by the Russian Foundation for Basic Research (project no. 03-05-64351), the Russian–German program "Laptev Sea System," funded by the Ministry of Science and Technology, and the NSF (USA) grant no. OP-99 86 826.

References

Anisimov MA and Tumskoi VE (2003) Ice beds in the island of Novaya Sibir' (Novosibirskie Islands, Russia). In: Proceedings of the International conference Kriosfera Zemli kak sreda zhizneobespecheniya (Earth Cryosphere as Life-Support System), Pushchino (Russia) (in Russian), pp 232–233

Balobaev VT (1991) Geotermiya merzloi zony litosfery Severa Azii (Geothermal Measurements in the Permafrost of Northern Asia) (in Russian). Nauka, Novisibirsk, p 193

Bauch HF, Muller-Lupp T, Taldenkova E (2001) Chronology of the Holocene transgression at the Northern Siberia margin. Global Planet Change 31:125–139

Chappell J, Omura A, Esat T, McCulloch M, Pandolfi J, Ota Y, Pillans B (1996) Reconciliation of late Quaternary sea level derived from coral terraces at Huon Peninsula with deep sea oxygen isotope records. Earth Planet Sci Lett 141:227–236

Chuvilin EM, Perlova EV, Makhonina NA, Yakushev VS (2000) Research of hydrate and ice formation in soils during cyclic fluctuations of temperature. In: Thimus JF (ed) Ground freezing 2000. Balkema, Rotterdam, pp 9–14

Creager JS, McManus DA (1967) Bottom sediments data from the continental shelf of the Chuckchi and Bering seas. Washington University Department of Oceanography Technical Report, vol 135, pp 343–351

Danilov ID, Komarov IA, Vlasenko AYu (1997) Dynamics of the cryolithosphere in the shelf-continent interaction zone within the last 25,000 years (by the example of East Siberian Sea) (in Russian). Earth Cryosphere 1(3):3–8

Danilov ID, Komaro IA, Vlasenko AYu (1998) Pleistocene–Holocene Permafrost of the East Siberian Eurasian Arctic shelf. In: Proceedings of the 7th international conference on permafrost, June 23–27, Yellowknife, Canada, pp 207–212

Danilov ID, Komarov IA, Vlasenko AYu (2000) Cryolithozone of the East Siberian Shelf in the Last 80 000 Years (in Russian). Earth Cryosphere 4(1):18–23

Delisle G (1998) Temporal variability of subsea permafrost and gas hydrate occurrences as a function of climate change in the Laptev Sea, Siberia. Polarforschung 68:221–226

Devyatkin VN (1993) Teplovoi potok kriolitozony Sibiri (Thermal Flux from the Cryolithozone of Siberia) (in Russian). Nauka, Novosbirsk, p 165

Dmitrenko IA, Hoelemann JA, Kirillov SA (2001) Thermal regime of the near-bottom layer of the Laptev Sea and the processes controlling it (in Russian). Earth Cryosphere 5(3):40–55

Drachev SS (1998) Laptev Sea rifted continental margin: modern knowledge and unsolved questions. Polarforschung 68:41–50

Drachev SS, Savostin LA, Bruni JE (1995) Structural pattern and tectonic history of the Laptev Sea region. Rep Polar Res 176:348–367

Drachev SS, Jonson GL, Laxon SW (1999) Main structural elements of eastern Arctic Continental Margin derived from satellite gravity and multichannel seismic reflection data. In: Kassens H, Bauch HA, Dmitrenko I, Eicken H, Hubberten H-W, Melles M, Thiede J, Timokhov L (eds) Land–Ocean systems in the Siberian Arctic: dynamics and history. Springer, Berlin Heidelberg New York, pp 667–682

Drachev SS, Kaul N, Beliaev VN (2003) Eurasia spreading basin to Laptev Shelf transition: structural pattern and heat flow. Geophys J Int 152:688–698

Duchkov AD (ed) (1985) Catalogue of geothermal heat flow data of Siberia (1966–1984) Institute of Geology and Geophysics of Siberian Branch of USSR Academia of Science (in Russian). Novosibirsk, p 82

Duchkuv AD and Sokolova LS (1985) Temperature of the lithosphere of Siberia according to geothermal data. Sovetskaia Geologi I Geophisika (in Russian). USSR Geology Geophisc 26:53–61

Fairbanks RJ (1989) A 17 000-years glacio-eustatic sea level record: influence of glacial melting rates on the Younger Dryas event and deep ocean circulation. Nature 342:637–642

Fartyshev AI (1993) Osobennosti pribrezhno-shel'fovoi kriolitopzony morya Laptevykh (Pecularities of Permafrost in the Shelf Zone of the Laptev Sea) (in Russian). SB Nauka Publisher, Novosibirsk, p 135

Franke D, Hinz K, Blok M, Drachev SS, Neben S, Kos'ko MK, Reichert Chr, Roester HA (1998) Tectonics of the Laptev Sea region in North-Eastern Siberia. Polarforschung 68:51–58

Franke D, Krueger F, Kling KD (2000) Tectonics of the Laptev Sea—Moma 'Rift' region: investigation with seismologic broadband data. J Seismology 4:99–116

Franke D, Hinz K, Oncken O (2001) The Laptev Sea rift. Mar Petrol Geol 18(10):1083–1127

Gavrilov AV, Tumskoi VE (2001) Evolution of the temperature of rocks in coastal lowlands of Yakutia in the middle and late Pleistocene (in Russian). Earth Cryosphere 4:3–16

Gavrilov AV, Tumskoi VE, Romanovskii NN (2000) Reconstruction of mean annual permafrost temperature dynamics in coastal lowlands and the Arctic Shelf of Yakutia within the last 400,000 years (in Russian). Earth Cryosphere 4(4):3–14

Gavrilov AV, Romanovskii NN, Romanovsky VE, Hubberten HW (2001) Offshore permafrost distribution and thickness in the eastern region of the Russian Arctic. In: Semiletov IP (ed) Changes in the atmosphere–land–sea system in the Amerasian Arctic (in Russian). In: Proceedings of the Arctic Regional Center Vladivostok, vol 3. pp 209–218

Gavrilov AV, Romanovskii NN, Romanovsky VE, Hubberten H-W, Tumskoy VE (2003) Reconstruction of ice complex remnants on the East Siberian Arctic Shelf. Permafrost Periglacial Processes 14:187–198

Geotermicheskay karta mira (Geothermal Map of the World, scale 1:45 M) (1988) Explanatory note (in Russian). VSEGEI, Leningrad, p 41

Glossary of Permafrost and Related Ground-Ice Terms (1988) National Research Council Canada. Technical Memorandum No.142, p 156

Grigor'ev NF (1966) Monogoletnemerzlye porody Primosrskoi zony Yakutii (Permafrost in the Coastal Zone of Yakutia) (in Russian). Nauka Publisher, Moscow, p 180

Grigoriev MN, Rachold V, Bolshiyanov DYu, Pfeiffer EM, Schirrmeister L, Wagner D, Hubberten H-W (eds) (2003) Russian–German Cooperation System Laptev Sea—the expedition lena 2002. Rep Polar Mar Res 466:341

Groisman AG (1985) Teplophisicheskie svoistva gazovih hydratov (Thermophysical properties of Gas Hydrates) (in Russian). Nauka, Novosibirsk, p 94

Hinz K, Delisle G, Block M (1998) Seismic evidence for the depth extend of permafrost in shelf sediments of the Laptev Sea, Russian Arctic? In: Proceedings of the 7th international conference on permafrost, June 23–27, Yellowknife, Canada, pp 453–457

Holmes ML, Creager JS (1974) Holocen history of the Laptev Sea Continental shelf. In: Herman Y (ed) Marine geology and oceanography. Springer, Berlin Heidelberg New York, pp 211–229

Hopkins DM (1976) History of sea-level changes in Beringia within the last 250,000 years, Beringiya v Kainozoe (Beringia in the Cenozoic) (in Russian). DVNC AN SSSR, Vladivostok, pp 9–27

Hubberten H-W, Romanovskii NN (1999) Recent approach to the problem "Paleoreconstruction of the climate-sea-land interaction" during Pleistocene–Holocene as a base for the field research and monitoring: Laptev Sea Region (in Russian). Abstracts, In: Conference"Monitoring of the Cryosphere", Pushchino, p 36

Hubberten H-W and Romanovskii NN (2000) Onshore and offshore permafrost of the Laptev Sea region during the Late Pleistocene–Holocene glacial-eustatic cycle. Polarforschung 68:227–230

Hubberten H-W, Romanovskii NN (2003) The main features of permafrost in the Laptev Sea region, Russia—a review. In: Proceedings of the 8th international conference on permafrost, 21–25 July 2003, Zurich, Switzerland, A.A. Balkema, Rotterdam, vol 1, pp 431–436

Ivanov VF (1982) Sea-level oscillations near the coasts of eastern Chukotka in the Late Pleistocene and Holocene. Kolebaniya urovnya morei i okeanov za 15 000 let (Fluctuations in the Level of Seas and Oceans within the Last 15 000 years) (in Russian). Nauka, Moscow, pp 190–195

Kaplina TN (1981) Late Cenozoic history of permafrost in the North of Yakutia, Istoriya razvitiya mnogoletnemerzlykh porof Evrazii (History of Permafrost in Eurasia) (in Russian). Nauka, Moscow, pp 153–181

Kassens H, Bauch HA, Dmitrenko I, Eicken H, Hubberten H-W, Melles M, Thiede J, Timokhov L (eds) (1999) Land–Ocean systems in the Siberian Arctic: dynamics and history. Springer, Berlin Heidelberg New York, p 711

Kholodov AL, Gavrilov AV, Romanovskii NN, and Hubberten H-W (1999) The results of modeling permafrost dynamics in coastal lowlands and within the Arctic Shelf for the last 400,000 years (in Russian). Earth Cryosphere 4(4):32–40

Khrutskii SF, Kondrat'eva KA, Rybakova NO (1977) The Section of Cenozoic Deposits in Grabens of the Primorpskii Fault Zone (Yana–Omoloi Interfluve) (in Russian), Merzlotnye issledovaniya, iss. vol XVI, MGU, Moscow, pp 89–108

Kuz'min MI, Karabanov EB, Kawai T, Williams D, Bychinskii VA, Kerber EV, Kravchinskii VA, Bezrukova EV, Prokopenko AA, Geletii VE, Kalmychkov GV, Goreglyad AV, Antipin VS, Khomotova MYu, Soshina NM, Ivanov EV, Khursevich GK, Tkachenko LL, Solotchina EP, Ioshida N, Gvozdkov AN (2001) Deep drilling on Lake Baikal: main results (in Russian). Geol Geophys 42:8–34

Lysak SV (1988) Geotermicheskii potok kontinental'nykh riftovykh zon (Geothermal Flux in Continental Rift Zones) (in Russian). Nauka Publisher, Novosibirsk, p 200

Neizvestnov YaV (1981) Permafrost and Geological Conditions of Arctic Shelves of the USSR, Krilitozona arkticheskogo basseina (Cryyolithozone of the Arctic Basin) (in Russian). Yakutsk, Publisher Inst. Merzlotovedeniya Sib. Otd. Akad Nauk SSSR, pp 18–28

Neizvestnov YaV, Voinov ON, Postnov IS (1976) Salt and Gas Composition of Deep Ground Water in Novosibirskie Islands and Adjacent Areas. Geologiya shel'fa vostochnosibirskikh morei (Shelf Geology for East Siberian Seas) (in Russian). Leningrad, Nauchno-Issled. Inst. Geology of Arctic and Antarctic Publisher, pp 78–89

Petit JR, Jouzel J, Raynaud D, Barkov NI, Barnola JM, Basile I, Bender M, Chappellaz J, Davis M, Delaygue G, Delmotte M, Kotlyakov VM, Legrand M, Lipenkov VY, Lorius C, Pepin L, Ritz C, Saltzmann E, Stievenard M (1999) Climate and atmospheric history of the past 420,000 years from the Vostok ice core, Antarctica. Nature 399:429–436

Pfeiffer E-M, Grigoriev MN (eds) (2002) Russian–German Cooperation SYSTEM LAPTEV SEA 2000: the expedition LENA 2001. Rep Polar Mar Res 426

Ponomarev VM (1937) Permafrost as seen from newest data (in Russian). Problemy sovetskoi geologii 7(4):27–34

Ponomarev VM (1960) Podzemnye vody na territorii s moshchnoi tolshchei mnogolenetnemerzlykh gornykh porod (Ground water in the areas with deep permafrost) (in Russian). Izd. Akad. Nauk SSSR, Moscow, p 200

Rachold V (2002) The modern and ancient terrestrial and coastal environment of the Laptev Sea region, Siberian Arctic—a preface. Polarforschung 70:1–2

Rachold V, Grigoriev MN (eds) (1999) Russian–German Cooperation SYSTEM LAPTEV SEA 2000: the Lena Delta 1998 expedition. Rep Polar Mar Res 316:259

Rachold V, Grigoriev MN (eds) (2000) Russian–German Cooperation SYSTEM LAPTEV SEA 2000: the expedition lena 1999 expedition. Rep Polar Mar Res 354:269

Rachold V, Grigoriev MN (eds) (2001) Russian–German Cooperation SYSTEM LAPTEV SEA 2000: the expedition LENA 2000. Rep Polar Mar Res 388:135

Romanovskii NN, Hubberten H-W (2001a) The formation and evolution of permafrost in the shelf and coastal lowlands (by the example of Laptev Sea Region) (in Russian). Izvest Akad Nauk ser Geography 3:15–28

Romanovskii NN, Hubberten H-W (2001b) Results of permafrost modeling of the lowlands and shelf of the Laptev Sea Region, Russia. Permafrost Periglacial Processes 12:191–202

Romanovskii NN, Gavrilov AV, Kholodov AL (1997a) Reconstruction of paleogeographic conditions in the late Pleistocene and Holocene glacioeustatic cycle for the Laptev Sea Shelf (in Russian). Earth Cryosphere 1(2):42–49

Romanovskii NN, Gavrilov AV, Pustovoit GV, Kholodov AL (1997b) Distribution of relic offshore permafrost in the Laptev Sea Shelf (in Russian). Earth Cryosphere 1(3):9–18

Romanovskii NN, Gavrilov AV, Kholodov AL (1998) The forecasting map of Laptev Sea Shelf Off-shore Permafrost. Permafrost. In: Proceedings of 7th international conference on permafrost, June 23–27, Yellowknife, Canada, pp 967–972

Romanovskii NN, Kholodov AL, Gavrilov AV, Tipenko GS, Hubberten H-W (1999) Permafrost thickness in the eastern part of the Laptev Sea shelf (results of modeling) (in Russian). Earth Cryosphere 4(2):22–32

Romanovskii NN, Hubberten H-W, Romanovsky VE, Kholodov AL (2003) Permafrost evolution under the influence of long-term climate fluctuation and glacio-eustatic sea-level variation: region of Laptev and East Siberian Seas, Russia. In: Proceedings of the 8th international conference on permafrost, 21–25 July 2003, Zurich, Switzerland, A.A. Balkema Publishers, vol 2, pp 983–988

Sekretov SB (1998) Petroleum potential of Laptev Sea basins:geological, tectonic and geodynamic factors. Polarforschung 68:179–186

Sekretov SB (1999) Eurasian Basin–Laptev Sea geodynamic system: tectonic and structural evolution. Polarforschung 69:51–54

Selivanov AO (1996) Izmeneniya urovnya Mirovogo okeana v pleistotsene-golotsene i razvitie morskikh beregov (Changes in Sea Level in the Pleistocene and Holocene and the Development of Sea Coasts) (in Russian). Nauka, Moscow, p 268

Sher AV (1984) The age of quaternary deposits in the Yana–Kolyma lowland and surrounding mountains (in Russian). Dokl Akad Nauk SSSR 278(3):708–713

Solov'ev VA (1981) Forecast of the relic offshore permafrost distribution (by the example of East Siberian Seas). Kriolitozona arkticheskogo she'lfa (cryolithozone of the Arctic Shelf) (in Russian), Yakutsk, Inst. Merzlotoved. Sibirsk. Otd. Akad, Nauk SSSR Publisher, pp 28–38

Solov'ev VA, Ginsburg GD, Telepnev EV, Mikhalyuk YuN (1987) Kriogeotermiya i gidraty prorodnogo gaza v nerdakh Severnogo Ledovitogo Okeana (Cryogeothermal Measurements and Hydrates of Natural Gases below the Arctic Ocean) (in Russian)

Tektonicheskaya karta morei Karskogo i Laptevykh i Severa Sibiri (Tectonic map of the Kara and Laptev Seas and the north of Siberia) (1998) (in Russian) Moscow, Inst. Litosfery okrainnykh i vnutrennikh morei RAN, Leningrad, PGO Sevmorgeologiya, p 127

Tipenko GS, Romanovskii NN, Kholodov AL (1999) Simulation of the offshore permafrost and gashydrate stability Zone of: mathematical solution, numerical realization, and preliminary results. Polarforschung 69:229–234

Veinbergs IG (1991) Ancient sea coasts of the USSR (peculiarities of distribution, genesis, and alteration stages) (in Russian), Author's abstract of Doctoral dissertation, Moscow State University., p 49

Zhigarev LA (1981) Regularities of the crylithozone formation in the Arctic Basin, Krilitozona arkticheskogo basseina (Cryyolithozone of the Arctic Basin) (in Russian). Yakutsk, Inst. Merzlotovedeniya Sib. Otd. Akad Nauk SSSR Publisher, pp 4–17

Zhigarev LA (1997) Okeanicheskaya kriolitozona (Oceanic Cryolithozone) (in Russian). Moscow State University Publisher, Moscow, p 318